Local Staging of Prostate Cancer with Endorectal MR Imaging: Correlation with Histopathology

Gerrit J. Jager[1]
Emiel T. G. Ruijter[2,3]
Christina A. van de Kaa[3]
Jean J.M.C.H. de la Rosette[2]
Gosse O.N. Oosterhof[2]
John R. Thornbury[4]
Jelle O. Barentsz[1]

OBJECTIVE. To evaluate the accuracy of MR imaging of the prostate with an endorectal surface coil in determining presence, localization, volume, and local stage of prostate carcinoma.

SUBJECTS AND METHODS. MR images of 34 patients with biopsy-proven cancer were correlated retrospectively with the histologic mappings of radical prostatectomy specimens. The volume and number of tumor lesions on MR images were calculated and compared with the surgical specimens used as the gold standard. Tumor stage based on MR imaging was compared with the pathologic stage according to the TNM classification. Predictive values were calculated separately for all lesions and for the lesions correctly localized with MR imaging.

RESULTS. MR imaging correctly depicted the location of 67% of the tumors. Twenty percent of the lesions depicted by MR imaging appeared to be false-positive errors. The tumors that were missed were located centrally and ventrally in the prostate. Tumor volume as shown by MR imaging was within a 25% range of the actual tumor volume in 10 cases, overestimated in 16 cases, and underestimated in eight cases. Histopathology showed capsular penetration in 12 of 34 patients (35%) and in 14 of 52 lesions (27%). Sensitivity, specificity, and positive predictive values were 43%, 84%, and 55%, respectively. Histologically, capsular penetration extended less than 1 mm into the periprostatic adipose tissue in seven patients. Sensitivity for capsular penetration less than 1 mm was 14%. Sensitivity for capsular penetration more than 1 mm was 71%. Accuracy for differentiating a pT2 from a pT3 tumor was 68%.

CONCLUSION. Results from this study indicate that the accuracy of the technique was not satisfactory for predicting actual tumor volume. Tumor detection and localization was more accurate in the peripheral zone than in the central zone. Accuracy was poor for detecting capsular penetration of less than 1 mm, but accuracy was much better for penetration of more than 1 mm. Because recent reports suggest that capsular penetration of less than 1 mm does not adversely affect surgical cure, MR imaging still may be practical in the selection of patients for radical prostatectomy.

AJR 1996;166:845–852

Received September 19, 1995; accepted after revision November 13, 1995.

[1]Department of Radiology, University Hospital Nijmegen, P.O. Box 9101, 6500 HB, Nijmegen, the Netherlands. Address correspondence to G. J. Jager.

[2]Department of Urology, University Hospital Nijmegen, P.O. Box 9101, 6500 HB, Nijmegen, the Netherlands.

[3]Department of Pathology, University Hospital Nijmegen, P.O. Box 9101, 6500 HB, Nijmegen, the Netherlands.

[4]Department of Radiology, University of Wisconsin-Madison, 185 Morgan Pl., Castle Rock, CO 80104.

0361–803X/96/1664–845

The incidence of prostate cancer is increasing. The disease trails only lung cancer as the leading cause of death in men [1]. Staging of prostate cancer is a systematic classification of the extent of disease based on clinical and pathologic criteria. Clinical stage is used to sort patients into comparable groups for definitive therapy, whereas pathologic stage is important in predicting prognosis and the need for additional therapy. Curative treatment is considered possible only if the tumor is confined to the prostate gland (stage ≤T2) [2]. Therefore, differentiating between a T2 and a T3 tumor is clinically important. On the other hand, several reports have stated that patients with minimal capsular penetration have a prognosis similar to that of patients whose tumors are completely confined to the prostatic capsule [3, 4].

Not established is what MR imaging technique results in the most accurate diagnosis and preoperative staging. Initially, the accuracy of body coil MR imaging with conventional spin-echo sequences was promising [5]. Body coil MR imaging has the advantage that pelvic bones and lymph nodes can also be evaluated during the

same session. However, the signal-to-noise ratio and the spatial resolution are too low to provide high-resolution images of the prostate [6].

With the recent development of an endorectal surface coil (ERC), the prostate and its surrounding structures are visualized much better [7]. With fast spin-echo techniques, T2-weighted images in three different planes are obtained in a shorter time with a higher resolution matrix and fewer motion artifacts than are images obtained with conventional spin-echo sequences [8]. The results suggested improved staging accuracy.

Several recent studies have reported the results of MR imaging with ERC technique imaging for staging prostate cancer [7, 9–16]. Accuracy levels ranged from 54% to 83%. In three of these studies, fast spin-echo MR images with an ERC were correlated with histopathologic mapping [12, 14, 16].

As an adjunct to staging, the volume of prostate cancer is also important for prognosis [17–19]. When tumor volume is smaller than 4 cc metastasis is highly unlikely, whereas when tumor volume exceeds 12 cc metastasis is highly likely [20]. MR sequences with standard body coil and conventional spin-echo techniques have not given accurate images for estimating tumor volume before surgery [5, 21–25]. However, fast spin-echo MR images obtained with a phased-array coil estimated tumor volume better [8].

In our study, we evaluate the diagnostic accuracy of MR imaging with fast spin-echo sequences that use an ERC to determine tumor presence, tumor volume, and the preoperative stage of prostate carcinoma. In addition, we identify common pitfalls of MR imaging interpretation and the correlation of MR images with pathology.

Subjects and Methods

Patient Population

The study population was 34 patients with needle biopsy–proven adenocarcinoma. We performed MR imaging that used an ERC technique and followed that with radical retropubic prostatectomy. Patients' mean age was 65 years old (range, 50–73 years old). When biopsies preceded MR imaging, the average time was 3 weeks. Patients underwent radical prostatectomy within 3 weeks of imaging. Patients who underwent MR imaging and then received hormonal treatment before surgery were excluded from this study. All patients had clinical T2–3 disease according to the TNM classification (Table 1) [26]. We detected no lymph-node metastases in frozen sections at laparoscopic or open lymph-node dissection that preceded the radical prostatectomy. Local staging by MR imaging was correct in 16 of 34 cases, or 47%, as confirmed by histopathologic examination.

MR Technique

All images were obtained using a 1.5-T Siemens SP system (Siemens, Erlangen, Germany), and a Medrad endorectal coil (Medrad, Pittsburgh, PA). We placed the coil with the patient in the lateral decubitus position and inflated the coil with 50–100 ml of air. Peristalsis was suppressed by administering 1 mg of glucagon intravenously. A tight band was wrapped around the patient's abdomen to decrease respiratory movement.

A sagittal T1-weighted localized image was obtained to confirm coil positioning and to select locations for the axial images. Axial T-1 weighted images (420/22 [TR/TE]) as well as axial, sagittal, and coronal fast spin-echo T2-weighted images (2940/160, echo-train length of 13) were performed. All examinations were performed using a 4- or 5-mm slice thickness with a 1- or 2-mm gap, 26-cm field of view, and a 512 × 216 matrix. An equalizing processing after application and a filter algorithm to compensate for near-field effect were also used. We also changed the phase-encoding gradient to decrease motion artifacts over the prostate. An examination usually lasted 30–45 min.

MR Imaging Examination

The MR images were retrospectively interpreted by a single reader, who had been interpreting MR examinations for prostate cancer and correlating the results with clinical and pathologic outcome for more than 2 years. The reader had no knowledge of the clinical find-

TABLE 1: 1992 Revision of TNM Classification [26]

Designation	Tumor Characteristics	No. of Cases	No. Identified by MR Imaging
TX	Not assessable	0	0
T0	Not evident	0	0
T1	Clinically apparent; not palpable or visible by imaging		
T1a	Found incidentally in 5% or less of tissue resected	0	0
T1b	Found incidentally in more than 5% of tissue resected	0	0
T1c	Identified by needle biopsy due to elevated serum prostate-specific antigen	0	0
T2	Palpable or visible by prostate imaging		
T2a	Involves half lobe or less	2	0
T2b	Involves more than half lobe but not both lobes	0	0
T2c	Involves both lobes	20	11
T3	Extends through capsule		
T3a	Found unilaterally	3	0
T3b	Found bilaterally	3	2
T3c	Invades seminal vesicles	6	3
T4	Fixed or invades other structures		
T4a	Invades bladder neck, external sphincter, or rectum	0	0
T4b	Invades levator muscles or is fixed to pelvic wall	0	0

ings, the PSA level, or the results of histopathologic examination or transrectal sonography. Image quality was recorded with special regard to motion artifacts. An image was considered to be of poor quality when degraded by motion artifacts. Good quality meant that these artifacts did not significantly degrade delineation of structures.

On T2-weighted images, an area in the peripheral zone with a low signal intensity when compared with the adjacent peripheral zone was considered to be a malignancy. Low-signal-intensity areas in the central zone were not interpreted as malignancy [27]. If a low-signal-intensity area showed high signal on the corresponding T1-weighted image, the area was considered to be a hematoma.

Tumors separated by more than 1 cm, without connection to another tumor in an adjacent section, were interpreted as separate tumor lesions. Tumor volume was calculated by the sum of tumor areas multiplied by slice thickness, including gaps between slices.

We used the following criteria to define capsular perforation: disruption of the prostatic capsule, infiltration of the periprostatic fat, low-signal-intensity stranding, and involvement of the neurovascular bundle. A bulge in the contour or capsular thickening was not interpreted as capsular perforation [9, 12]. Abnormally low signal intensity within the lumen of the seminal vesicle or focal thickening of the seminal wall was interpreted as seminal vesicle invasion [9]. Final staging was recorded according to the TNM classification (Table 1) [26].

Pathologic Examination

The prostatectomy specimens were in toto fixed overnight in a solution of 4% neutral buffered formalin. Step-sections were made at 4-mm intervals in a plane parallel to the base of the prostate, which corresponded to the slices used on MR imaging. After separating the step-sections into right and left halves, all sections were routinely embedded in paraffin. Tissue sections of 5 μm were prepared and stained with hematoxylin and eosin. Regions representing cancer were outlined on the glass cover and retraced onto a diagram of the axial histologic sections that extended from the base to the apex of the prostate. To estimate tumor volume, the sum of the cancer areas on all sections was multiplied by 4 mm (slice thickness). The volume was then multiplied by a factor of 1.1 to correct for tissue shrinkage due to fixation. Length and depth of penetration through the capsule and involvement of each seminal vesicle were recorded. Definitive staging was performed with the TNM classification [26].

Data Analysis

A radiologist and a pathologist analyzed the correlation of MR imaging findings and histopathology. The MR images were correlated with tumor maps that were based on the histopathologic sections. Tumor localization, number of tumors, tumor volume, status of the prostate capsule, involvement of each seminal vesicle, and definitive stage were evaluated.

To offset the bias of incorrectly identified lesions (false positives), we analyzed matched lesions (true positives). A tumor location was considered to match if the tumor was present in the same craniocaudal third of the prostate (proximal, mid, or distal) and the tumor was localized in the same quadrant, regardless of the size of the lesion. Penetration through the capsule was compared for each tumor lesion.

Results

The endorectal coil was well tolerated by all patients. In 28 patients, images obtained with the ERC provided detailed visualization of the prostate, prostatic capsule, and periprostatic structures, including the seminal vesicles. In six patients, image quality was poor because of motion artifacts caused by bowel motion (n = 5) or because of upward migration of the endorectal coil (n = 1). Minor image degradation resulted from biopsy hematoma, high signal intensity close to the ERC (near-field effect), and shallow penetration depth of the ERC; however, image quality remained good.

Pitfalls in Correlating MR Images with Histopathologic Findings

The correlation between MR images and tumor maps based on histopathology was difficult in almost all patients. The most caudal section of MR images was 0.5–1.5 cm lower than the section representing the apex in the prostatectomy specimen. Also, the angle by which the sections were cut was never exactly the same for either technique (difference, 5–15°). Furthermore, the shape of the prostate changed after fixation. Also making correlation difficult was the fact that the prostate tumors were markedly irregular and often demonstrated fingerlike projections with ill-defined margins that did not display on MR images of 4 or 5 mm (whereas the histologic sections were only 4 μm thick). We tried to overcome these problems by using tumor maps, which gave a good three-dimensional picture of the prostate. We also used our definition of a matched lesion.

Number and Localization of Tumor Lesions

A total of 44 separate tumor lesions were visualized with MR imaging, and 52 were found on histopathologic examination of 34 patients (mean number of tumors, 1.5; range, 1–3). Thirty-four tumors were defined matched lesions (Fig. 1). In 10 false-positive lesions identified by MR imaging, histopathology showed adjacent cystic changes in six cases. In four other false-positive lesions identified by MR imaging, histopathology failed to show an explanation for the low signal intensity.

MR imaging correctly depicted the location of 67% of the tumors. Twenty-two percent of the lesions depicted by MR appeared to be false-positive errors. Fourteen of the 18

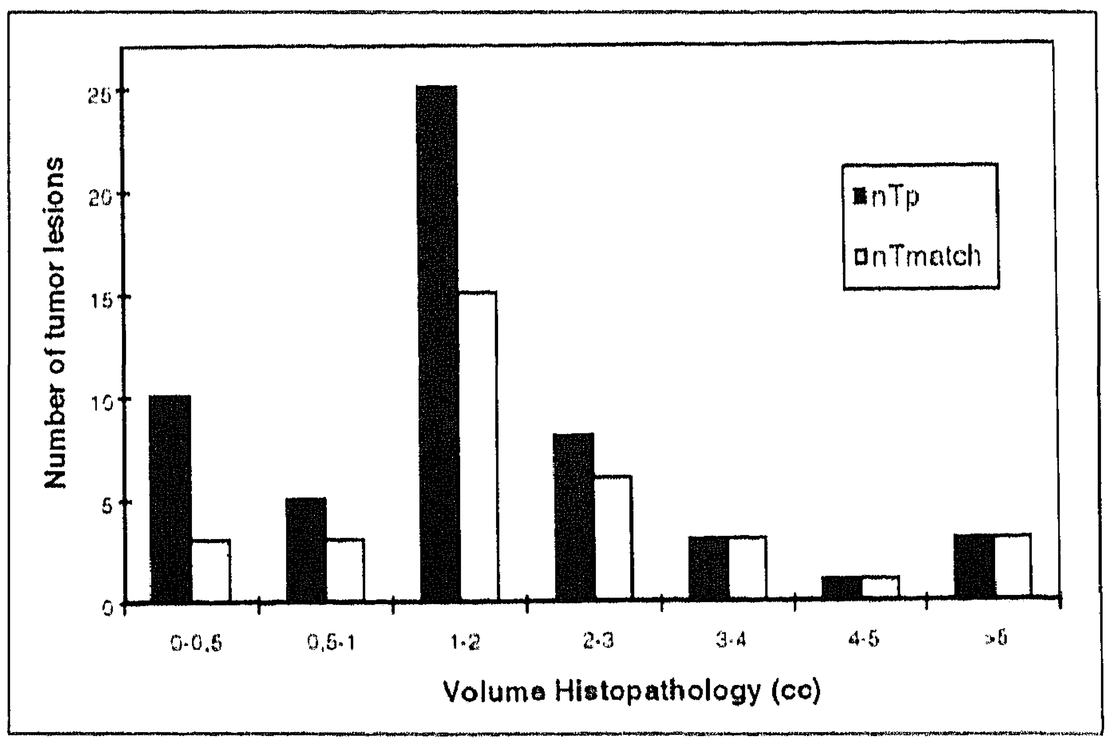

Fig. 1.—Bar graph shows distribution of lesions determined with histopathology (*solid bar*) ranged in order of actual tumor volume and degree of match lesions (*open bar*). Tumors less than 2 cc easily remain undetected with MR imaging.

tumors that were missed were located in the central or ventral part of the prostate.

Tumor Volume

The accuracy of MR imaging in predicting tumor volume is presented in Figure 2.

The mean volume of 44 tumor lesions captured on imaging with ERC was 2.3 cc (range, 0.25–11.6 cc). The mean volume of 52 histopathologically detected lesions was 1.5 cc (range, 0.4–7.2 cc). When we compared only matched lesions, the mean volume was 2.6 cc by MR imaging with ERC and 1.8 cc by histopathology. In seven matched lesions, the tumor volume estimated by MR imaging fell within a 25% range of the actual volume. In 19 other cases, MR imaging overestimated the actual tumor volume by more than 25% (Fig. 3), and in eight other cases, the underestimation by MR imaging exceeded 25%. In the latter group, 50% of the lesions were located in the central or ventral part of the prostate.

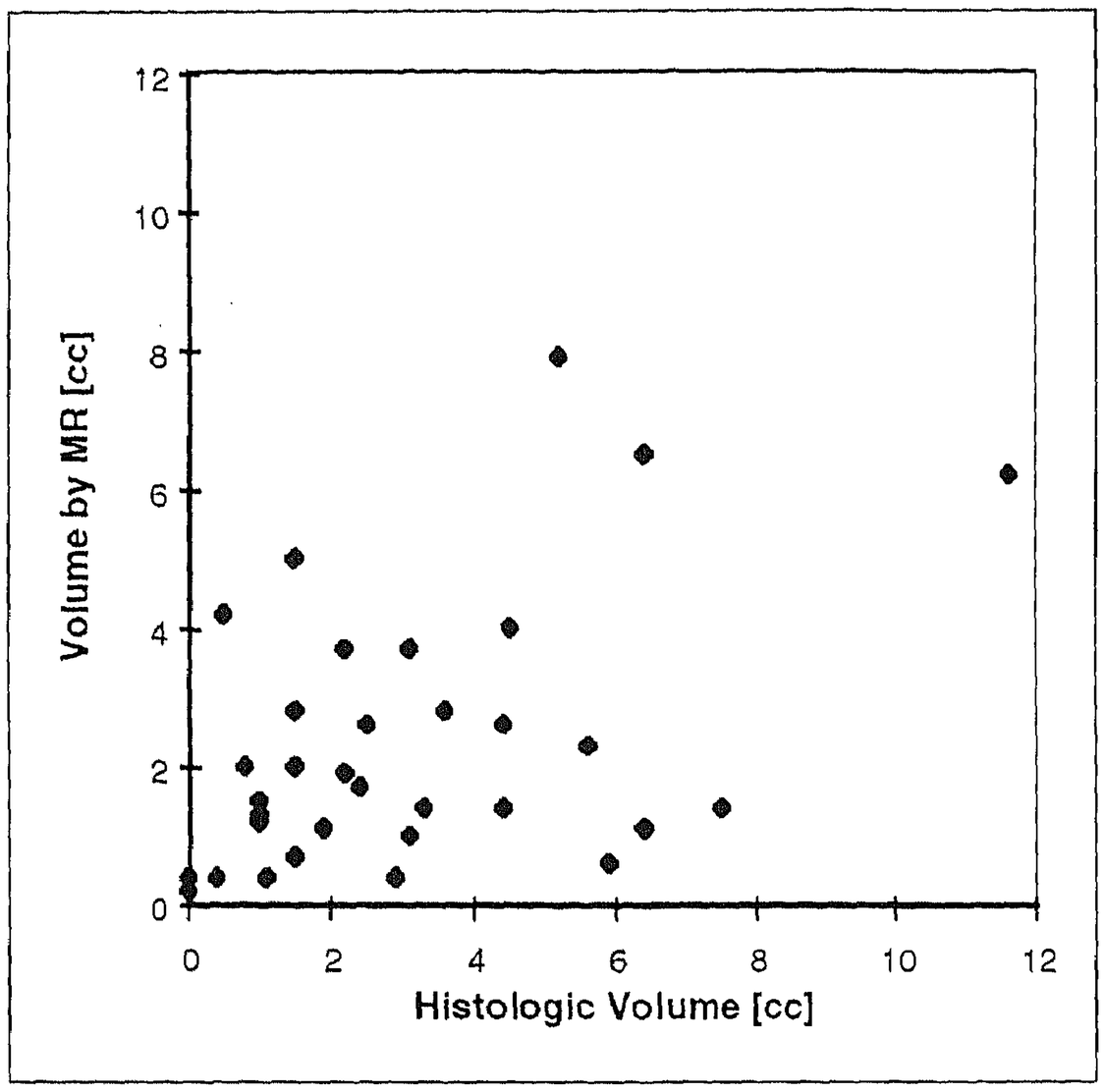

Fig. 2.—Scatter plot shows poor correlation between volume determined by MR imaging and actual tumor volume.

Capsular Penetration

In 11 of 44 (25%) lesions identified by MR imaging, evidence of capsular penetration was stated. In 14 of 52 (27%) lesions detected by histopathology, capsular penetration was present. False-positive capsular penetration was present in four matched and in one false-positive lesion. Three cases of false-positive capsular penetration occurred in MR imaging examinations with poor image quality because of motion artifacts.

Histologically, seven patients had capsular penetration with a width of more than 5 mm; MR imaging correctly identified the capsular penetration in four of them. Seven patients had capsular penetration with a width of less than 5 mm; MR imaging correctly identified two of them. Histologically, capsular penetration extended less than 1 mm into the periprostatic adipose tissue in seven lesions; 1–3 mm in six; and more than 3 mm in one (Fig. 4). Sensitivity of MR for depicting capsular penetration into the periprostatic tissue was 14% when that penetration was less than 1 mm, 67% when 1–3 mm, and 100% when more than 3 mm (Fig. 5).

The capsular bulge sign was not used because it may lead to false-positive findings [9]. Capsular bulge was found in four cases, once in a true-positive T2 tumor, once in a false-negative T3 tumor, and twice in (for other reasons) true-positive T3 tumors. Thus, this criterion would not change the overall accuracy for capsular penetration.

Five patients also had positive surgical margins. However, because the surgeon incised the capsule, capsular penetration could not be evaluated in those sections. Overall figures are given in Tables 2 and 3.

Invasion of Seminal Vesicles

All 68 seminal vesicles were visualized. MR imaging showed tumor invasion in 11 seminal vesicles of eight patients, of which four lesions were confirmed on histopathology. In 51 out of 57 seminal vesicles, invasion was correctly excluded with MR imaging. The sensitivity was 36% (4 of 11). The specificity was 89% (51 of 57). The positive predictive value was 36% (4 of 11). The results are presented in Tables 4 and 5. The seven false-positive seminal vesicles showed no abnormalities in the corresponding histopathologic sections. In particular, fibrosis, inflammatory infiltrate, amyloid depositions, and blood were excluded. Eight vesicles showed focal thickening of the tubular wall. Only four of them were true-positive (Figs. 6 and 7).

Staging Prostate Cancer

For all patients, we evaluated final staging of prostate cancer by comparing MR images with pathologic appearances (Table 1). With the TNM classification, staging was correct in 15 out of 34 (44%) patients. When staging was limited to depict locally advanced disease, (≥T3, formerly Jewitt stage C) sensitivity, specificity, accuracy, and positive predictive values of MR staging were 67%, 68%, 68%, and 53%, respectively (Table 6).

One patient who had stage pT3b (bilateral capsular penetration) disease was staged with MR imaging as mT3c without capsular perforation. Another patient was correctly staged as mT3 because of a false-positive and a false-negative lesion; thus, staging by MR imaging in these patients was correct for an incorrect reason.

Discussion

Motion artifacts were the primary cause of low-quality images in five examinations (14%). Also, of these five cases, three had false-positive capsular penetration. Little is reported in the literature about significant motion artifacts and the use of ERC. However, with fast spin-echo imaging and a pelvic phased-array multicoil, one study reported sig-

Fig. 3.—Overestimating of tumor volume and underestimating of number of tumors in 62-year-old man.

A, Axial fast-spin-echo T2-weighted image shows zone of decreased intensity on right (*arrows*), interpreted as carcinoma. Estimated volume was 3.3 cc. At pathologic examination, tumor location was almost symmetrically bilateral. Calculated tumor volume both right and left was 0.7 cc.

B, Photograph of histopathologic section shows two small tumor foci (*arrows*) on right side.

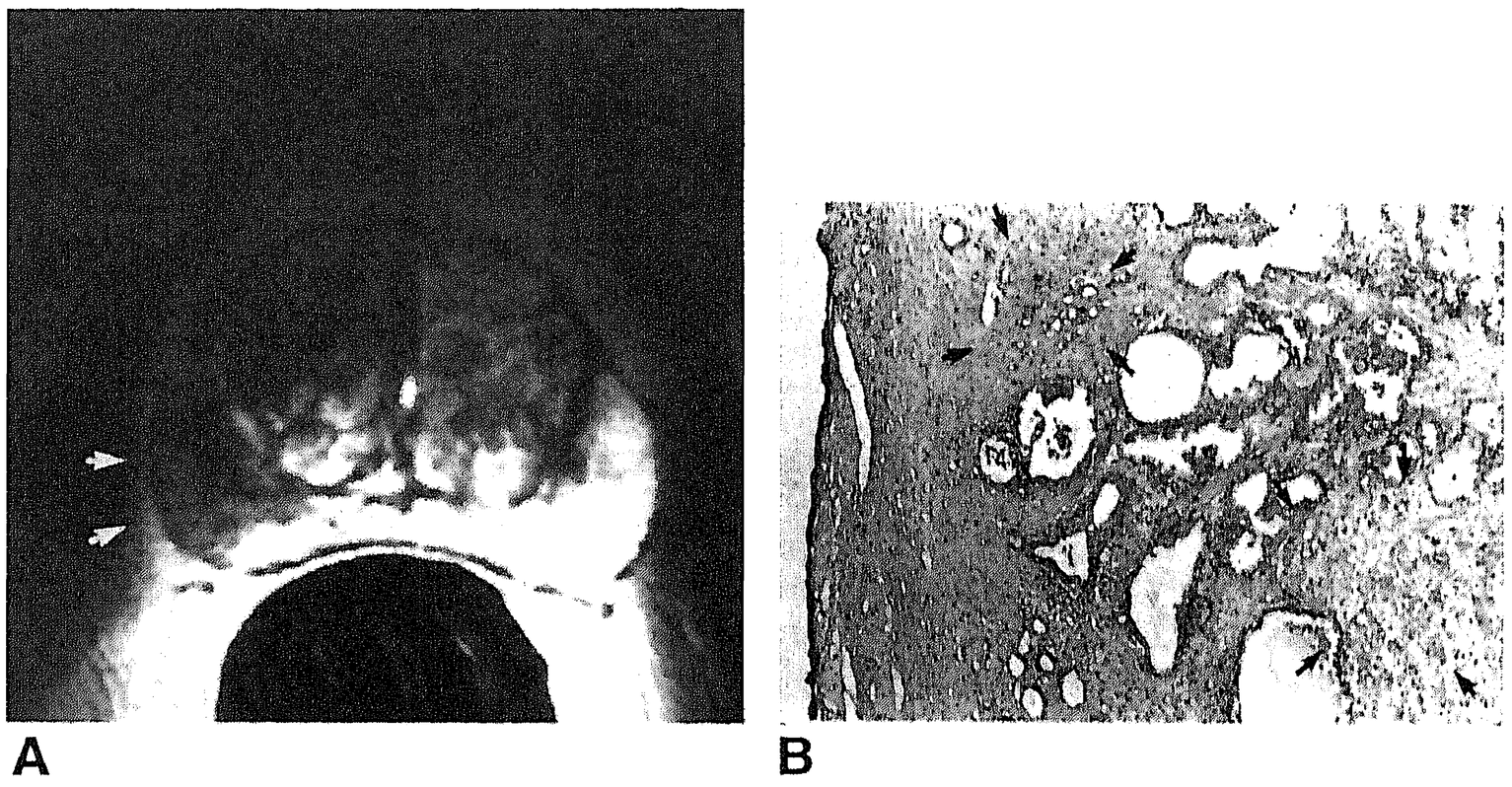

Fig. 4.—Good correlation between MR imaging and pathology in 57-year-old patient.

A, Axial T2-weighted fast spin-echo image shows gross extracapsular tumoral involvement of extraprostatic tissue (*arrows*).

B, Photograph of pathologic specimen shows close match for status of capsule and tumor volume (*arrows*).

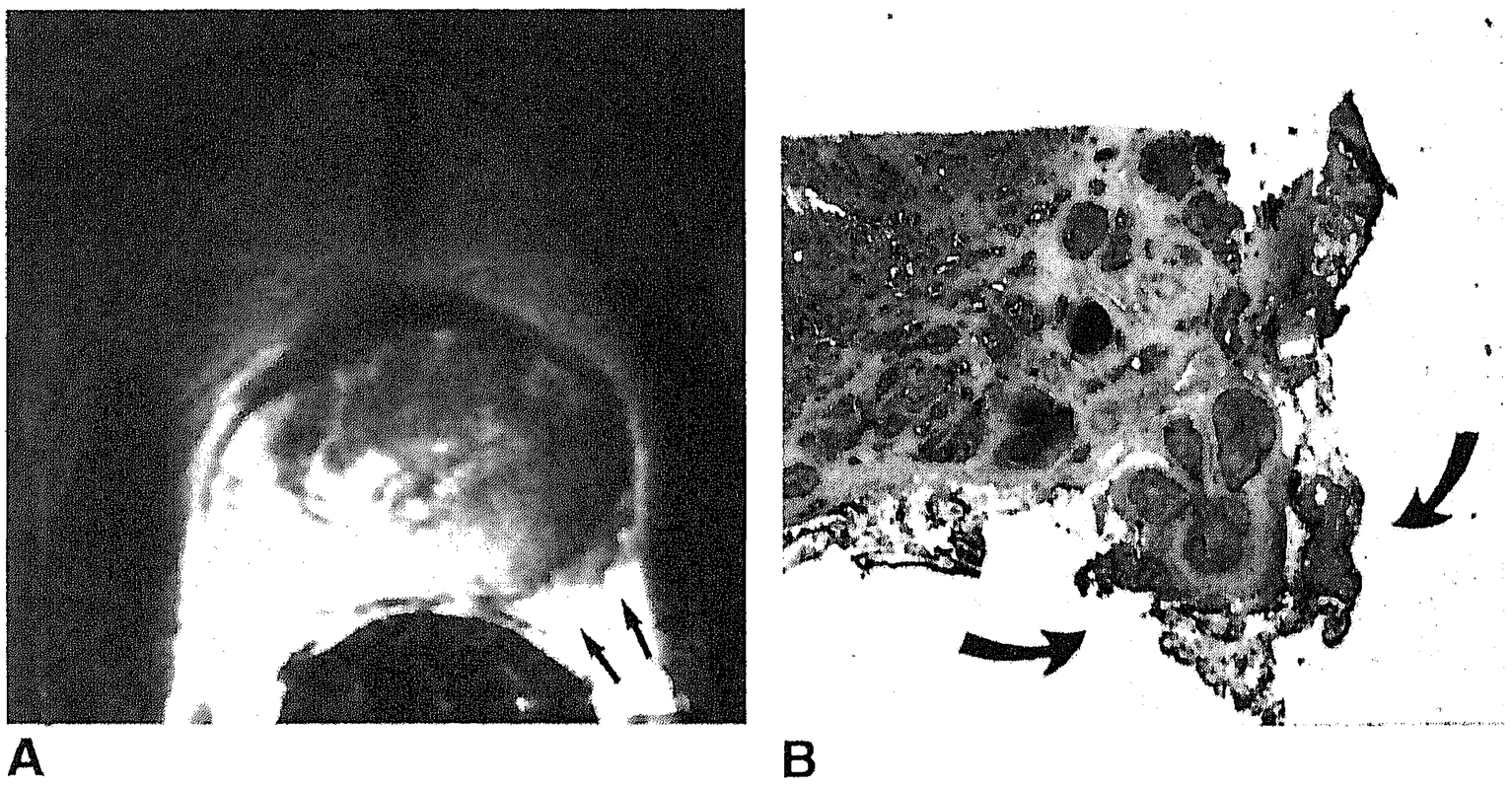

nificant motion artifacts in up to 45% of examinations when glucagon was not used versus 7% with glucagon [8].

Number and Localization

In our study, correlation was good between number and localization of tumors. The positive predictive value and sensitivity level were relatively high, comparable to that of other studies [12, 14, 25, 28]. We confirmed that tumors located ventrally and centrally on histopathologic examination are pitfalls for false-negative tumors. Carter et al. [28] found a sensitivity of 15% in detecting anterior tumors, a percentage considerably lower than they achieved in detecting posterior tumors (85%). Outwater et al. [12] did not identify any of 29 central gland tumors and 41 of 56 (73%) peripheral tumors on MR imaging that used an ERC technique.

Causes for false-positive findings that are reported in the literature include hyperplasia, prostatitis, postbiopsy hemorrhage with blood in the extracellular methemoglobin state, and areas of cystic change [25]. Cystic change increases the signal intensity of the peripheral zone, resulting in a relatively low signal intensity compared with adjacent areas of normal prostate, which may be confused with malignant lesions. We found neither histologic evidence of hematoma nor other pathologic changes in areas defined as hematoma on T1-weighted images. These findings concur with a study in which 27 false-positive lesions that corresponded with areas of hemorrhage on T1-weighted images did not show any pathologic substrate, especially no evidence of hemorrhage [14]. Also, the pathologist cited by Tempany et al. [16] stated that the effects of hemorrhage and biopsy are difficult to quantify and cannot always be identified at pathologic analysis.

Tumor Volume

Tumor volume is a known predictor of pathologic stage [17]. With a tumor volume larger than 12 cc, extraprostatic spread of disease has likely occurred, whereas tumors smaller than 4 cc are usually locally confined [20]. Tumor volume is reported to correlate more closely with progression than with capsular penetration [19].

We found a poor correlation between tumor volumes calculated from MR images and those found at pathologic examination. Although pathologic examination frequently showed tumor extension into the central and ventral part of the prostate, MR images overestimated mean volume in all lesions

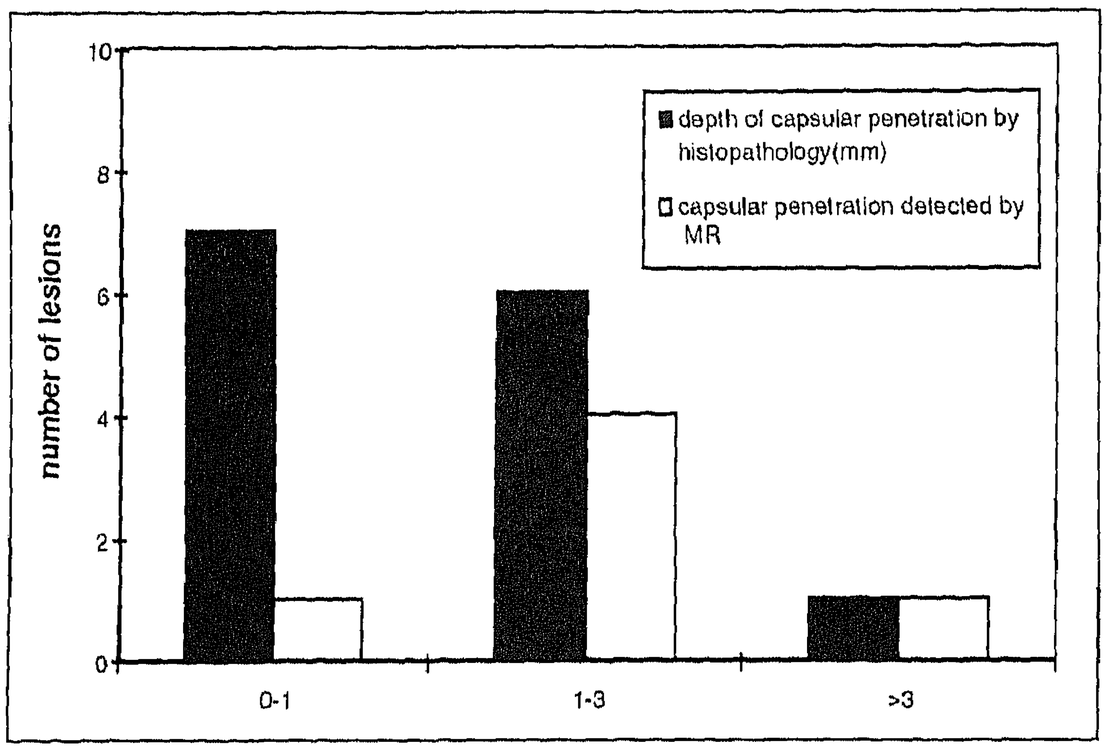

Fig. 5.—Bar graph shows relation of detecting capsular penetration with MR imaging (*open bar*), to depth of tumor invasion (mm) on histopathology (*solid bar*). Sensitivity was 14%, 67%, and 100% for capsular penetration of less than 1 mm, between 1 and 3 mm, and more than 3 mm, respectively.

TABLE 2: Results of MR Imaging for Capsular Penetration with All Histologic Lesions

MR Findings	Histopathology		
	Present	Absent	Total
Present	6	5	11
Absent	8	33	41
Total	14	38	52

Note.—Sensitivity = 42%; specificity = 87%; accuracy = 75%; positive predictive value = 55%.

TABLE 3: Results of MR Imaging for Capsular Penetration with Matched Lesions

MR Findings	Histopathology		
	Present	Absent	Total
Present	6	4	10
Absent	5	19	24
Total	11	23	34

Note.—Sensitivity = 55%; specificity = 85%; accuracy = 74%; positive predictive value = 60%.

and in matched lesions. We could not identify any reasons for this overestimate of tumor volume by MR imaging.

Studies performed with MR imaging using body coils reported a poor correlation between tumor volume as depicted on MR imaging and the volume calculated from the pathologic specimen [5, 21, 22, 24]. No studies in the literature used an ERC, although one study was performed with an external array coil and fast spin-echo technique [25]. This study reported a significant correlation between tumor volume calculated with MR images and that of the pathological specimen ($r = .81$, $p < .001$), but accuracy was not enough to be helpful in making clinical decisions.

To meet the problems of low predictive values for detecting tumors and estimating their volumes, studies have been performed that evaluated IV contrast medium–enhanced T1-weighted images [11, 29]. However, improvement over T2-weighted FSE images was not observed. Nonetheless, the report of one study that used dynamic, single-slice T1-weighted technique after IV contrast medium with a high-time resolution (one image/sec) suggests that a better delineation of prostate cancer detection, volume, and staging may be possible with MR imaging [30].

Capsular Penetration

Accuracy for capsular penetration in our study was low for matched lesions (55%) because capsular penetration was less than 3 mm in all but one case. On matched lesions we found no relation between the width or length of the capsule at pathologic examination and the staging accuracy with MR imaging. Five patients with positive surgical margins due to incision by the surgeon through the capsule were classified as T2 because penetration through the prostatic capsule could not be confirmed. Of these five, MR classification was T2 in three cases and T3 in two cases.

In a recent overview, Schiebler et al. [31] stated that body coil MR imaging proves unsatisfactory at detecting capsular penetration due to the limited spatial resolution of the imaging technique. MR imaging that uses ERC technique is reported to more reliably identify the prostatic capsule [15]. Detection of capsular penetration with MR imaging with ERC technique had a sensitivity of 67% compared with body coil MR imaging, which had a sensitivity of 44% in the same patient cohort. However, the results of recent studies of MR imaging with ERC technique showed limited accuracy for detecting capsular penetration [9, 12, 14, 16]. For example, Tempany et al. [16] reported that accuracy rates of MR imaging with ERC technique for detecting capsular penetration from different institutions ranged from 33% to 54%, which is less accurate than conventional body-coil MR imaging.

These conflicting findings may result from the lack of highly specific and sensitive diagnostic criteria for capsular penetration. One study has evaluated six different diagnostic criteria for capsular penetration [12]. The positive predictive value of each individual sign ranged from a minimum of 4% for capsular thickening to a maximum of 34% for extracapsular tumor.

It should be noted that focal penetration probably has a prognosis comparable to T2 tumors [3]. Therefore, only identification of deeper penetration may be of clinical importance [32].

Seminal Vesicle Invasion

The accuracy for detecting seminal vesicle involvement in our series agreed with that in other series. A high specificity (85–97%) and a low sensitivity (21–63%) [9, 14, 16] were reported. In our study, the figures were 82% and 50%, respectively. Although we could not explain the false-positive findings in the histopathology, low signal intensity of the seminal vesicles on T2-weighted images can be caused by amyloid deposits [33] or seminal vesicles that contain stones

TABLE 4: Results of MR Imaging for Seminal Vesical Invasion

MR Findings	Histopathology		
	Present	Absent	Total
Present	4	7	11
Absent	7	51	58
Total	11	58	69

Note.—Sensitivity = 36%; specificity = 89%; accuracy = 79%; positive predictive value = 36%.

TABLE 5: Results of MR Imaging for Seminal Vesical Invasion for Each Patient

MR Findings	Histopathology		
	Present	Absent	Total
Present	3	5	8
Absent	6	20	26
Total	9	25	34

Note.—Sensitivity = 33%; specificity = 80%; accuracy = 68%; positive predictive value = 38%.

or blood [31]. Focal tubular thickening proved unreliable in predicting seminal vesicle involvement in our series.

Overall Staging

In our study, staging according to the TNM classification was correct in 47% of the patients. Accuracy for differentiating a T2 from a T3 tumor was 68%. Except for Hricak et al. [34], other studies restricted staging to differentiating T2 from T3. The first series on imaging with an ERC reported an 82% accuracy rate, which was a 16% improvement over body coil staging with the same cohort of patients [15]. Recent series reported an overall accuracy of 54–68% for MR imaging that used an ERC [9, 12, 14, 16]. Accuracy in prospective studies (51%) is considerable lower than in retrospective studies (67%) [14, 35].

TABLE 6: Results of Detecting Extraprostatic Disease (≥T3)

MR Findings	Histopathology		
	$p \leq$ T2	$p \geq$ T3	Total
m ≤ T2	15	4	19
m ≥ T3	7	8	15
Total	22	12	34

Note.—Sensitivity ≥T3 = 67%; specificity ≥T3 = 68%; accuracy = 68%; negative predictive value ≥T3 = 79%; positive predictive value ≥T3 = 53%.

The patient group in our study was limited to the patients who underwent radical prostatectomy. We also perform MR imaging on the prostates of patients who did not undergo radical prostatectomy because of positive lymph nodes or because of the overall staging results. The accuracy rate might well be different if this group were also included.

Difficulties in Evaluating the Literature

The continuous, rapid technical development of image sequences and coil design such as pelvic phased-array and integrated endorectal pelvic phased-array coils [34] can produce a wide divergence of image quality. Imaging with the combination of an ERC and a phased-array multicoil is now advocated as the most powerful tool.

In addition, a broad spectrum of diagnostic signs (often indirect) and differently defined criteria for capsular penetration make metaanalysis of the literature difficult. For example, authors of one report changed image sequences, surface coils, and diagnostic criteria during the study [14]. Also, not all reports are blinded in the same way. Accuracy levels may be pushed higher when clinical data (prostate-specific antigen, prior histories of prostatitis, and locations of the positive biopsy findings) are integrated with interpretation of the images as recommended by Schiebler et al. [31]. Furthermore, it is often difficult to assess the extent to which information gained from MR imaging was used in patient management (verification bias) [36, 37]. In our institution, the prevalence of T3 tumors at opera-

Fig. 6.—Axial T2-weighted fast spin-echo image of 67-year-old patient shows thickening of wall of seminal vesicles (*arrows*). Seminal vesicle invasion was confirmed at pathologic examination.

6

Fig. 7.—Axial T2-weighted fast-spin-echo image of 63-year-old patient shows more pronounced tubular thickening (*arrows*), but seminal vesicle invasion was not present at pathologic examination.

7

tion has decreased from 63% in the study by Jager et al. [10] to 35% in this study. Because prostate cancer often leads to surgery at an early stage [38], correction for verification bias remains impossible. For these reasons, comparison of our presented figures to those of other studies is difficult.

Conclusion

Although MR imaging using an ERC with a fast spin echo was not highly accurate in predicting definitive tumor volume or definitive stage, the technique may prove helpful when selecting patients for definitive therapy because small capsular penetration of less than 1 mm—often not detected by MR imaging—does not rule out radical prostatectomy. Follow-up studies are necessary to evaluate the effect of understaging minimal capsular penetration. In our series, overstaging occurred frequently in cases with low-quality images due, at least in part, to motion artifacts. Because tumor volume is likely to be more important than focal capsular penetration, the accuracy of assessing tumor volume must improve. Dynamic, single-slice T1-weighted technique that uses an IV contrast medium with high-time resolution (1 image/sec) shows promise of improved accuracy [30].

Because the value of MR imaging is not yet established and because the results of studies are difficult to compare, we conclude that those who perform MR imaging in cases of prostate cancer should determine their own standard of accuracy by carefully comparing their imaging results with histopathologic findings.

ACKNOWLEDGMENTS

We thank D. J. Ruiter and J. A. Schalken for helpful comments.

REFERENCES

1. Borings CC, Squires TS, Tong T. Cancer statistics, 1993. *CA Cancer J Clin* **1993**;43:7–26
2. Steinfield AD. Questions regarding the treatment of localized prostate cancer. *Radiology* **1992**;184:593–598
3. Epstein JI, Carmichael MJ, Pizov MJ, Walsh PC. Influence of capsular penetration on progression following radical prostatectomy: a study of 196 cases with long-term followup. *J Urol* **1993**;150:135–141
4. Epstein JI, Pizov G, Walsh PC. Correlation of pathologic findings with progression after radical retropubic prostatectomy. *Cancer* **1993**;71:3582–3593
5. Bezzi M, Kressel HY, Allen KS, et al. Prostatic carcinoma: staging with MR imaging at 1.5 T. *Radiology* **1988**;169:339–346
6. Rifkin MD, Zerhouni EA, Gatsonis CA, et al. Comparison of magnetic resonance imaging and ultrasonography in staging early prostate cancer: results of a multi-institutional cooperative trial. *N Engl J Med* **1990**;323:621–626
7. Schnall MD, Lenkinski RE, Pollack HM, Imai Y, Kressel HY. Prostate: MR imaging with an endorectal surface coil. *Radiology* **1989**;172:570–574
8. Kier R, Wain S, Troiano R. Fast spin-echo MR imaging of the pelvis obtained with a phased-array coil: value in localizing and staging prostatic carcinoma. *AJR* **1993**;161:601–606
9. Chelsky MJ, Schnall MD, Seidmon EJ, Pollack HM. Use of endorectal surface coil magnetic resonance imaging for local staging of prostate cancer. *J Urol* **1993**;150:391–395
10. Jager GJ, Barentsz JO, Rosette de la JJMCH, Rosenbusch G. Preliminary results of endorectal surface coil magnetic resonance imaging for local staging of prostate cancer. *Radiologe* **1994**;34:129–133
11. Mirowitz SA. Seminal vesicles: biopsy related hemorrhage simulating tumor invasion at endorectal MR imaging. *Radiology* **1992**;185:373–376
12. Outwater E, Petersen RO, Siegelman ES, Gomella LG, Chernesky CE, Mitchell DG. Prostate carcinoma: assessment of diagnostic criteria for capsular penetration on endorectal coil MR images. *Radiology* **1994**;193:333–339
13. Parivar F, Rajanayagam V, Waluch V, Eto RT, Jones LW, Ross BD. Endorectal surface coil MR imaging of prostatic carcinoma with the inversion-recovery sequence. *J Magn Reson Imaging* **1991**;1:657–664
14. Quinn SF, Franzini DA, Demlow TA, et al. MR imaging of prostate cancer with an endorectal surface coil technique: correlation with whole-mount specimens. *Radiology* **1994**;190:323–327
15. Schnall MD, Imai Y, Tomaszewski JE, Pollack HM, Lenkinski RE, Kressel HY. Prostate cancer: local staging with endorectal surface coil MR imaging. *Radiology* **1991**;178:797–802
16. Tempany CMC, Zhou X, Zerhouni EA, et al. Staging of prostate cancer: results of Radiology Diagnostic Oncology Group project comparison of three MR imaging techniques. *Radiology* **1994**;192:47–54
17. Bostwick DG, Graham SD, Napalkov P, et al. Staging of early prostate cancer: a proposed tumor volume–based prognostic index. *Urology* **1993**;41:403–411
18. Stamey TA, Freiha JE, McNeal JE, Redwine E, Whittemore AS, Schmidt HP. Localized prostate cancer: relationship of tumor volume to clinical significance for treatment of prostate cancer. *Cancer* **1993**; 71[suppl]:933–938
19. McNeal JE, Villers A, Redwine E, Freiha FS, Stamey TA. Capsular penetration in prostate cancer: significance for natural history and treatment. *Am J Surg Pathol* **1990**;14:240–247
20. McNeal JE. Cancer volume and site of origin of adenocarcinoma of the prostate: relationship to local and distant spread. *Hum Pathol* **1992**; 23:258–266
21. Kahn T, Bürrig K, Schmitz-Drager B, Lewin JS, Fürst G, Modder U. Prostatic carcinoma and benign prostatic hyperplasia: MR imaging with histopathologic correlation. *Radiology* **1989**;173:847–851
22. McSherry SA, Levy F, Schiebler ML, Keefe B, Dent GA, Mohler JL. Preoperative prediction of pathological tumor volume and stage in clinically localized prostate cancer: comparison of digital rectal examination, transrectal ultrasonography and magnetic resonance imaging. *J Urol* **1991**;146:85–89
23. Outwater E, Schiebler ML, Tomaszewski JE, Schnall MD, Kressel HY. Mucinous carcinoma involving the prostate: atypical findings at MR imaging. *J Magn Reson Imaging* **1992**;2:597–600
24. Quint LE, Van Erp JS, Bland PH, et al. Prostate cancer: correlation of MR images with tissue optical density at pathologic examination. *Radiology* **1991**;179:837–842
25. Sommer FG, Nghiem HV, Herfkens R, McNeal JE, Low RN. Determining the volume of prostatic carcinoma: value of MR imaging with an external-array coil. *AJR* **1993**;161:81–86
26. Schroeder FH, Hermanek P, Denis L, Fair WR, Gospodarowicz MK, Pavone-Macaluso M. The TNM classification of prostate cancer. *Prostate* **1992**;4[suppl]:129–138
27. Schiebler ML, Tomaszewski JE, Bezzi M, et al. Prostatic carcinoma and benign prostatic hyperplasia: correlation of high-resolution MR and histopathologic findings. *Radiology* **1989**;172:131–137
28. Carter HB, Brem RF, Tempany CMC, et al. Nonpalpable prostate cancer: detection with MR imaging. *Radiology* **1991**;178:523–525
29. Sommer FG, Nghiem HV, Herfkens R, McNeal JE. Gadolinium-enhanced MRI of the abnormal prostate. *Magn Reson Imaging* **1993**;11:941–948
30. Jager GJ, Barentsz JO, de la Rosette JJMCH, Peters H, Hanselaar A, Oosterhof GON. Value of dynamic subtraction turboFlash MR imaging in prostate cancer (abstr). *Radiology* **1994**;193:316
31. Schiebler ML, Schnall MD, Pollack HM, et al. Current role of MR imaging in the staging of adenocarcinoma of the prostate. *Radiology* **1993**;189:339–352
32. Langlotz CP, Schnall MD, Malkowicz JB, Tomaszewski JE. Prediction of subsequent prostate carcinoma recurrence with preoperative staging with MR imaging: results of 3-year follow-up (abstr). *Radiology* **1994**;193:316
33. Ramchandani P, Schnall MD, LiVolsi VA, Tomaszewski JE, Pollack HM. Senile amyloidosis of the seminal vesicles mimicking metastatic spread of prostatic carcinoma on MR images. *AJR* **1993**;161:99–100
34. Hricak H, White S, Vigneron DB, et al. Carcinoma of the prostate gland: MR imaging with pelvic phased-array coils versus integrated endorectal-pelvic phased-array coils. *Radiology* **1994**;193:703–709
35. Demlow TA, Quinn SF, Franzini DA, Rosencranz DR, Szumowski J, Kim J. MR imaging of the prostate with endorectal surface coil technique and whole mount correlation (abstr). *Radiology* **1993**;189:251
36. Greenes RA, Begg CB. Assessment of diagnostic technologies: methodology for unbiased estimation from samples of selectively verified patients. *Invest Radiol* **1985**;20:751–756
37. Langlotz CP, Schnall MD, Pollack H. Staging of prostatic cancer: accuracy of MR imaging. *Radiology* **1995**;194:645–646
38. Lu-Yao GL, Greenberg ER. Changes in prostate cancer incidence and treatment in USA. *Lancet* **1994**;343:251–254